Available online at www.sciencedirect.com

SciVerse ScienceDirect

Ceramics International 38 (2012) 1341–1345

CERAMICS INTERNATIONAL

www.elsevier.com/locate/ceramint

Effects of HCl concentration on the growth and negative thermal expansion property of the ZrW_2O_8 nanorods

Hongfei Liu [a,*], Zhiping Zhang [b], Wei Zhang [c], Xiaobing Chen [c]

[a] Testing Center of Yang zhou University, Yang zhou 225009, PR China
[b] Department of Electrical and Mechanical Engineering, Jianghai College, Yang zhou 225009, PR China
[c] School of Physics Science and Technology, Yang zhou University, Yang zhou 225009, PR China

Received 23 July 2011; received in revised form 3 September 2011; accepted 3 September 2011
Available online 10 September 2011

Abstract

A kind of negative thermal expansion ZrW_2O_8 nanorods were synthesized using a hydrothermal method, followed with a post-annealing at 570 °C for 2 h. Effects of HCl concentration on the microstructure, morphology and negative thermal expansion property in resulting ZrW_2O_8 powders were investigated by X-ray diffraction (XRD) and transmission electron microscope (TEM). Results indicate that the formation of the precursor $ZrW_2O_7(OH)_2(H_2O)_2$ significantly depends on the HCl concentration, and the precursors $ZrW_2O_7(OH)_2(H_2O)_2$ can form in the 2–8 mol/L HCl solution. With increasing the concentration of the HCl solutions from 2 to 8 mol/L, the rod-like ZrW_2O_8 particles become more homogeneous, and the average dimension change from 10 μm × 0.5 μm to 700 nm × 50 nm. All the ZrW_2O_8 powders obtained in different conditions exhibit negative thermal expansion property, and the average negative thermal expansion coefficients from 15 °C to 600 °C decrease gradually with the increasing HCl concentration.

Keywords: Negative thermal expansion; Zirconium tungstate; Hydrothermal synthesis

1. Introduction

Negative thermal expansion (NTE) materials have attracted widespread interest due to their potential application over the last decade. While most materials expand with increasing temperatures, NTE materials contract upon heating. This makes them fascinating as fillers for use in composites, where they can mix with the positive thermal expansion materials to form various materials with controlled thermal expansion, being positive, negative or even zero. To date, cubic zirconium tungstate (ZrW_2O_8) has been considered one of the most promising NTE material. Due to its strong isotropic NTE property (-8.9×10^{-6} °C^{-1}) over its entire stability temperature range from −273 °C to 770 °C [1,2].

The conventional synthesis of ZrW_2O_8 used sintering of mixed powders of WO_3 and ZrO_2 at 1200 °C for several days with intermediate grindings, followed by rapid quenching in water [3–8]. The quenching step is necessary to avoid decomposition into binary oxides, as ZrW_2O_8 is only thermodynamically stable between 1105 °C and 1257 °C and metastable below 770 °C [9]. This method has several problems, such as the volatilization of WO_3, decomposition into WO_3 and ZrO_2 between 770 °C and 1105 °C, and the ZrW_2O_8 powders with inhomogeneous and large particle morphologies. The preparation of high quality composites requires a homogeneous distribution of filler particles, making small particles with uniform particle morphologies favorable for such applications. Two routes have been proposed to prepare nanosized ZrW_2O_8 particles, including sol–gel method [10,11] and hydrothermal synthesis [12,13]. These wet chemical methods often give access to small particles with uniform particle morphologies. Sol–gel route can reduce the heat-treatment temperature. However, the solution usually is aged and gelatinized for several weeks, and furthermore, the obtained ZrW_2O_8 particles are highly agglomerated. It is necessary to overcome this agglomeration problem, as it interferes with the preparation of high quality homogeneous composites. Compared with the conventional solid state

* Corresponding author. Tel.: +86 514 87979022; fax: +86 514 87979244.
E-mail address: liuhf@yzu.edu.cn (H. Liu).

0272-8842/$36.00
doi:10.1016/j.ceramint.2011.09.010

reaction and sol–gel route, the hydrothermal route presents many benefits such as use of mild temperature, elimination of high-temperature calcinations and removing aggregates, which is widely applied to synthesize powders at low temperatures. There are several papers reporting the hydrothermal synthesis of ZrW_2O_8. The ZrW_2O_8 is accessible by dehydration of a precursor, $ZrW_2O_7(OH)_2(H_2O)_2$, most previously reported synthesis of $ZrW_2O_7(OH)_2(H_2O)_2$ were carries out by hydrothermal treatment in HCl solution, but lack of series research on the influences of HCl concentration on the microstructures, particle sizes, morphologies, especially the NTE properties of the resulting products ZrW_2O_8. The former researches reported mainly focus on the effects of different acids, chloride ion concentration and alcohols on the preparation of the ZrW_2O_8 by hydrothermal method [12–16].

In this work, ZrW_2O_8 powders were synthesized using hydrothermal route in HCl solution with different concentration. We also report a detailed study on the effects of HCl concentration on the microstructure, particle size, morphology, especially the NTE property of the resulting ZrW_2O_8.

2. Experimental

All the chemical reagents were of analytical grade purity without further purification. In the typical procedure, zirconium oxynitrate [$ZrO(NO_3)_2{\cdot}5H_2O$] and ammonium tungstate [$N_5H_{37}W_6O_{24}{\cdot}H_2O$] were dissolved separately in distilled water according to the molar ratio of Zr:W = 1:2. The Zr solution was added slowly into the W solution under vigorous stirring. After stirring and heating at 80 °C for 2 h, 1, 2, 4, 6, 8, 10, 12 mol/L HCl solution were, respectively, added into the mixture and the stirring was continued. After 3 h, a homogenous mixture was formed. The mixture was finally poured into a Teflon-lined Parr bomb and heated at 180 °C for 15 h. Then the product was centrifuged, washed with distilled H_2O, and dried at 60 °C. To obtain ZrW_2O_8 powders, the resulting precursor was heat treated at 570 °C for 2 h.

The resulting products were characterized by powder X-ray diffraction using Cu Kα radiation (λ = 0.15418 nm) with 40 kV/200 mA (D/max2500, Rigaku). In situ X-ray diffraction measurements were used to characterize the resulting products with a scan speed of 2° (2θ) min^{-1} at 15, 100, 150, 200, 300, 400, 500 and 600 °C. The lattice constants of the products obtained at different temperatures were calculated by powder X software. The particle morphology and size were observed with the Holland Tecnai-12 transmission electron microscope (TEM) at an accelerating voltage of 120 kV.

3. Results and discussion

The crystal structures of the precursors and resulting powders were investigated by XRD experiments. Fig. 1 shows the typical XRD patterns of the precursors synthesized in HCl solutions with different concentrations (1, 2, 4, 6, 8, 10 and 12 mol/L). As one can see in Fig. 1, the precursors synthesized in 2, 4, 6 and 8 mol/L HCl solutions have almost the same XRD patterns, indicating that the same products were obtained, and

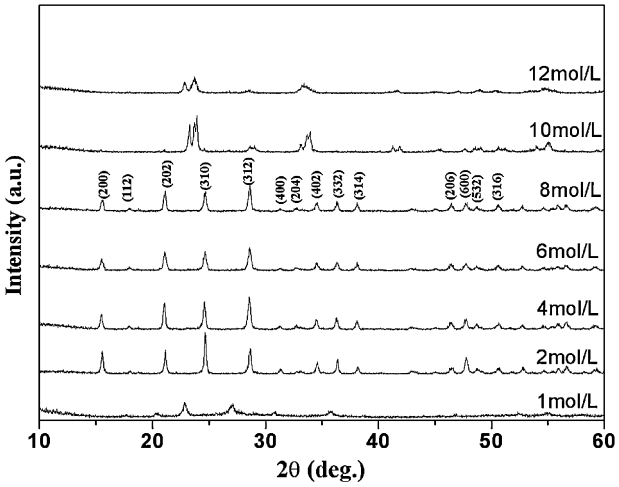

Fig. 1. XRD patterns of the precursors prepared in HCl solutions with different concentrations (C_{HCl} = 1, 2, 4, 6, 8, 10 and 12 mol/L).

all the XRD patterns of these precursors are in good agreement with that of $ZrW_2O_7(OH)_2(H_2O)_2$ (JCPDS28-1500), and the indices of crystallographic plane of the $ZrW_2O_7(OH)_2(H_2O)_2$ are also shown in Fig. 1. However, with further increase of the concentration of the HCl solutions, the resulting products synthesized in 10 and 12 mol/L HCl solutions mainly are WO_3 (JCPDS20-1324), it is probably because the concentration of the HCl solutions is too high to form the precursor $ZrW_2O_7(OH)_2(H_2O)_2$. In the hydrothermal synthesis, the following reactions may take place [16]:

$$ZrO^{2+} + (x+1)H_2O \rightarrow ZrO_2{\cdot}xH_2O + 2H^+ \quad (1)$$

$$WO_4{}^{2-} + 2H^+ + (y-1)H_2O \rightarrow WO_3{\cdot}yH_2O \quad (2)$$

$$ZrO_2{\cdot}xH_2O + WO_3{\cdot}yH_2O \rightarrow ZrW_2O_7(OH)_2(H_2O)_2 + (x+2y-3)H_2O \quad (3)$$

According to the above reactions, it can be seen that this reaction system has a close relationship with the acidity. When the concentrations of the HCl solutions increased (≥10 mol/L), it will promote the ammonium tungstate to hydrolyze and restrain the zirconium oxynitrate from hydrolyzing, so the resulting products synthesized in 10 and 12 mol/L HCl solutions mainly are WO_3. While the concentration of the HCl solution is too low (≤1 mol/L), the crystallized precursor $ZrW_2O_7(OH)_2(H_2O)_2$ cannot form. The product synthesized in 1 mol/L HCl solution shows an amorphous phase, which is similar to that reported by Xing et al. [14].

$ZrW_2O_7(OH)_2(H_2O)_2$ is an intermediate of the final product ZrW_2O_8. Based on our previous research on the TG-DSC of the $ZrW_2O_7(OH)_2(H_2O)_2$ [12], in this work, the heat-treatment temperature is chosen at 570 °C for 2 h.

$$ZrW_2O_7(OH)_2(H_2O)_2 \rightarrow ZrW_2O_8 + 3H_2O\uparrow \quad (4)$$

After heat-treatment at 570 °C for 2 h, the XRD pattern of resulting powder synthesized in 2 mol/L HCl solution is shown in Fig. 2(b), and the XRD pattern of its precursor is also given in

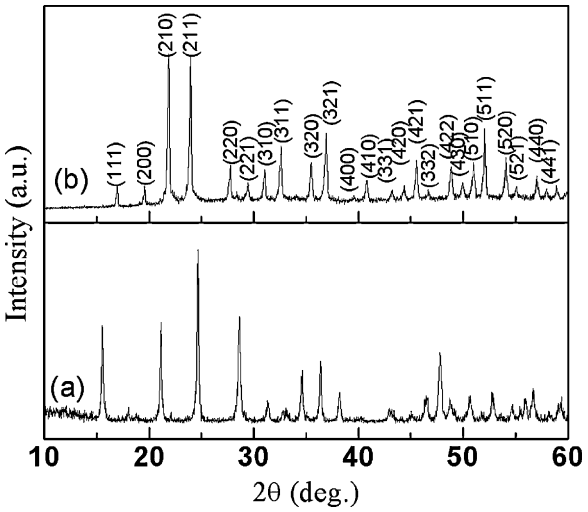

Fig. 2. XRD patterns of the precursor $ZrW_2O_7(OH)_2(H_2O)_2$ prepared in 2 mol/L HCl solution and the product ZrW_2O_8 post-annealed at 570 °C for 2 h.

Fig. 2(a). It can be seen that both the precursor and the heat-treated product are showing high and sharp diffraction peaks which indicates the good crystallinity of the specimens. The peak positions of the heat-treated product are well indexed to cubic ZrW_2O_8 (JCPDS 50-1868). And the other resulting products synthesized in 4, 6 and 8 mol/L HCl solutions also have the same XRD results. However, after heat-treatment, the precursors synthesized in 1, 10 and 12 mol/L HCl solutions all change into the mixed powders of ZrO_2 and WO_3. According to the XRD results discussed above, it reveals that the HCl concentration have a large effect on the formation of crystallized precursor $ZrW_2O_7(OH)_2(H_2O)_2$. In our experiment, it is found that the crystallized precursor $ZrW_2O_7(OH)_2(H_2O)_2$ can be obtained in the HCl solutions with the concentration between 2 mol/L and 8 mol/L.

Fig. 3 shows the TEM images of ZrW_2O_8 powders synthesized in 2, 4, 6 and 8 mol/L HCl solutions by hydrothermal route. All the ZrW_2O_8 powders obtained in different conditions show rod-like appearances. In Fig. 3(a), it can be seen that the ZrW_2O_8 rods synthesized in 2 mol/L HCl solutions are inhomogeneous, the big rod is about 10 μm in length and 0.5 μm in width and small one is about 2 μm in length and 50 nm in width. When the concentration of HCl solution increased, the rod-like ZrW_2O_8 particles become more homogeneous. The magnitudes of the ZrW_2O_8 rods synthesized in 4 and 6 mol/L HCl solutions are about 1.5 μm in length and 120 nm in width (see Fig. 3(b) and (c)), When the concentration

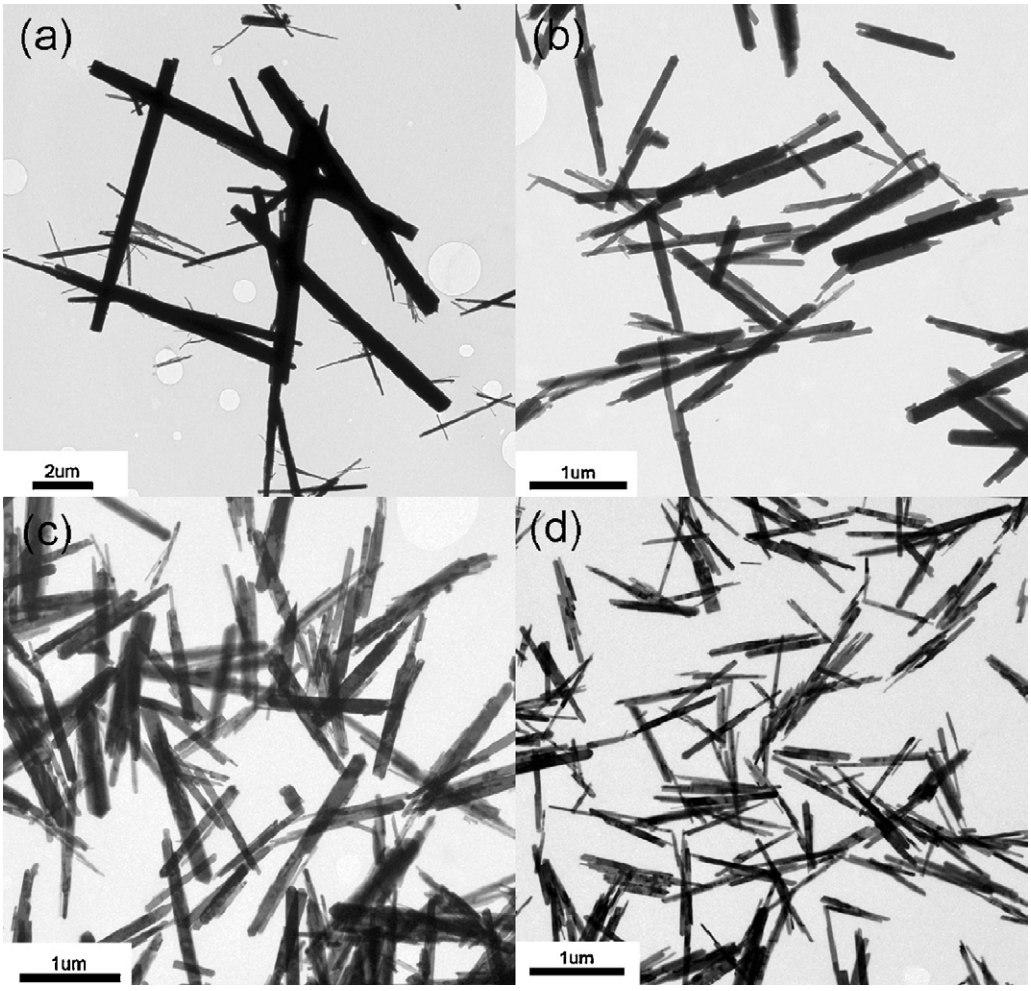

Fig. 3. TEM images of the ZrW_2O_8 particles prepared in HCl solutions with different concentrations: (a) 2 mol/L; (b) 4 mol/L; (c) 6 mol/L; (d) 8 mol/L.

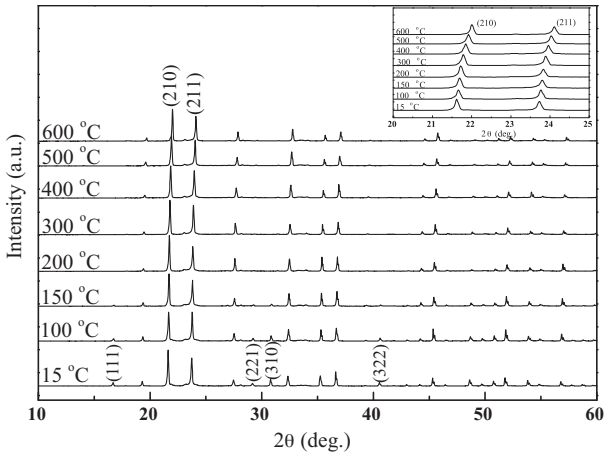

Fig. 4. XRD patterns of the ZrW_2O_8 powders prepared in 2 mol/L HCl solution characterized at different temperatures.

of HCl solution is 8 mol/L, the obtained ZrW_2O_8 particles are nanorod-like with average length of 700 nm and width of 50 nm. From the TEM results, it can be concluded that all the ZrW_2O_8 particles crystallized in rod-like appearances. With the increase of the concentration of HCl solution from 2 to 8 mol/L, the magnitudes of the ZrW_2O_8 rods decrease from micron to nanometer level and the morphologies of the particles become more homogeneous.

The concentration of the HCl solution plays an important role in the growth of ZrW_2O_8 by hydrothermal route. To further investigate the effects of the HCl concentration on the NTE properties of the obtained ZrW_2O_8 powders synthesized in different conditions (2, 4, 6 and 8 mol/L), all the NTE coefficients of ZrW_2O_8 powders were measured using in-site X-ray diffraction at different temperatures and then calculated by the cell parameter calculation method [17]. Fig. 4 shows the high temperature XRD patterns of the resulting ZrW_2O_8 powders (synthesized in 2 mol/L HCl solutions) characterized at various temperatures. From the graph, the peaks shift to higher diffraction angle with the increasing temperature, which can be found obviously from the inset in Fig. 4. Due to the cubic

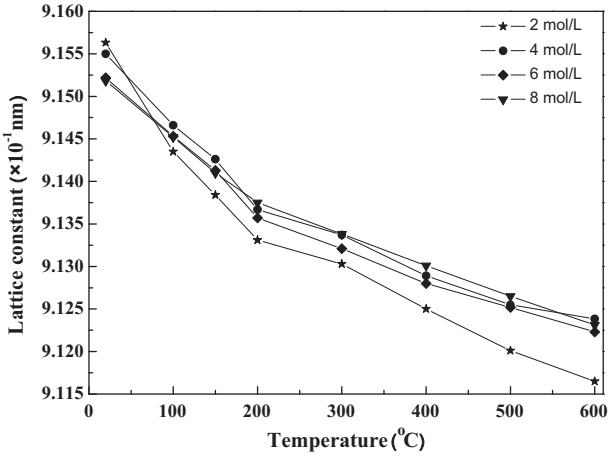

Fig. 5. The lattice constants depended on the temperatures for different specimens.

Table 1
NTE coefficients ($\times 10^{-6}$ °C $^{-1}$) of ZrW_2O_8 powders prepared in HCl solutions with different concentrations.

Concentration of HCl solution (mol/L)	Temperature range		
	15–200 °C	200–600 °C	15–600 °C
2	−14.03	−5.07	−6.73
4	−10.91	−3.61	−5.63
6	−9.86	−3.52	−5.42
8	−8.75	−3.90	−5.11

structure of the ZrW_2O_8, when the diffraction angle increases, value of *d* decreases in contrast, which lead to the decreasing of the lattice constants and contracting of the cell volume of ZrW_2O_8 by increasing temperatures. This indicates that the cubic ZrW_2O_8 powders show NTE property, attributed to the rigid unit mode of its framework structure and the liberation of the WO_4 unit with the unshared vertex [18–20]. In Fig. 4, the (1 1 1), (2 2 1), (3 1 0) and (3 2 2) peaks were observed in the XRD pattern below 200 °C, whereas they disappeared above 200 °C, which is due to the structure phase transition. The low-temperature phase ($P2_13$) transited to the high temperature phase (Pa $\overline{3}$). Between 150 °C and 200 °C, the structure of ZrW_2O_8 underwent an α to β structure phase transition, which is consistent with Refs. [21–25]. Other ZrW_2O_8 powders synthesized in 4, 6 and 8 mol/L HCl solutions also have the same phenomenon discussed above.

Fig. 5 depicts the lattice constants of ZrW_2O_8 depending on the temperatures. It is obvious that the lattice constants decrease with the increasing temperatures, which also indicates that NTE nature of the obtained ZrW_2O_8. After linear fitting, the NTE coefficients of ZrW_2O_8 synthesized in different HCl solutions are shown in Table 1. The NTE coefficients of all the α-phase ZrW_2O_8 (temperature from 15 °C to 200 °C) obtained in different conditions are lager than those of β-phase ZrW_2O_8 (temperature from 200 °C to 600 °C). With the increase of the concentration of HCl solutions, the average NTE coefficients of the ZrW_2O_8 powders in the temperature range from 15 °C to 600 °C decrease gradually. The concentration of the HCl solutions has some effects on the NTE property and which might be caused by the different microstructures. Further work is in the progress to investigate the formation mechanism in detail.

4. Conclusions

The rod-like ZrW_2O_8 powders were synthesized using a hydrothermal route. The influences of HCl concentrations on the growth and NTE property of ZrW_2O_8 were studied. To obtain the crystalline precursor $ZrW_2O_7(OH)_2(H_2O)_2$, the concentration of the HCl solution should be approximately kept between 2 and 8 mol/L. As the HCl concentration increases from 2 to 8 mol/L, the magnitudes of the ZrW_2O_8 rods become more homogeneous, and the increasing concentration also gives a reduction in particle size from 10 μm × 0.5 μm to 700 nm × 50 nm. Meanwhile, all the resulting ZrW_2O_8 powders show NTE properties and average NTE coefficients

from 15 °C to 600 °C decrease gradually with the increasing HCl concentrations.

Acknowledgments

The authors thank the Nation Natural Science Foundation of China (No. 50372027), the Nature Science Foundation for Key Basic Research of Jiangsu Higher Education Institution of China (No. 06KJA43010), Yang zhou University Development Foundation for Talents (No. 0274640015427) and Yang zhou University Science and Technique Innovation Foundation (No. 2010CXJ081).

References

[1] T.A. Mary, J.S.O. Evans, T. Vogt, A.W. Sleight, Negative thermal expansion from 0.3 K to 1050 K in ZrW_2O_8, Science 272 (1996) 90–92.
[2] J.S.O. Evans, T.A. Mary, T. Vogt, M.A. Subramanian, A.W. Sleight, Negative thermal expansion in ZrW_2O_8 and HfW_2O_8, Chem. Mater. 8 (1996) 2809–2823.
[3] S. Nishiiyama, T. Hayashi, T. Hattori, Synthesis of ZrW_2O_8 by quick cooling and measurement of negative thermal expansion of the sintered bodies, J. Alloys Compd. 417 (2006) 187–189.
[4] J.C. Chen, G.C. Huang, C. Hu, J.P. Weng, Synthesis of negative-thermal-expansion ZrW_2O_8 substrates, Scripta Mater 49 (2003) 261–266.
[5] G.R. Kowach, Growth of single crystals of ZrW_2O_8, J. Cryst. Growth 212 (2000) 167–172.
[6] J. Yang, Y.S. Yang, Q.Q. Liu, G.F. Xu, X.N. Cheng, Preparation of negative thermal expansion ZrW_2O_8 powders and its application in polyimide/ZrW_2O_8 composites, J. Mater. Sci. Technol. 26 (2010) 665–668.
[7] H.F. Liu, Z.P. Zhang, W. Zhang, X.B. Chen, X.N. Cheng, Negative thermal expansion ZrW_2O_8 thin films prepared by pulsed laser deposition, Surf. Coat. Technol. 205 (2011) 5073–5076.
[8] E.J. Liang, Y. Liang, Y. Zhao, J. Liu, Y.J. Jiang, Low-frequency phonon modes and negative thermal expansion in $A(MO_4)_2$ (A = Zr, Hf and M = W, Mo) by Raman and terahertz time-domain spectroscopy, J. Phys. Chem. A 112 (2008) 12582–12587.
[9] L.L.Y. Chang, M.G. Scroger, B. Philips, Condensed phase relations in the systems ZrO_2–WO_2–WO_3 and HfO_2–WO_2–WO_3, J. Am. Ceram. Soc. 50 (1967) 211–215.
[10] A.P. Wilkinson, C. Lind, S. Pattanaik, A new polymorph of ZrW_2O_8 prepared using nonhydrolytic sol–gel chemistry, Chem. Mater. 11 (1999) 101–108.
[11] K. Kanamori, T. Kineri, R. Fukuda, K. Nishio, A. Yasumori, Preparation and formation mechanism of ZrW_2O_8 by Sol–Gel process, J. Am. Ceram. Soc. 90 (2008) 3542–3545.
[12] X.J. Sun, J. Yang, Q.Q. Liu, X.N. Cheng, Influence of sodium dodecyl benzene sulfonate (SDBS) on the morphology and negative thermal expansion property of ZrW_2O_8 powders synthesized by hydrothermal method, J. Alloys Compd. 481 (2009) 668–672.
[13] N.A. Banek, H.I. Baiz, A. Latigo, C. Lind, Autohydration of nanosized cubic zirconium tungstate, J. Am. Chem. Soc. 132 (2010) 8278–8279.
[14] X.R. Xing, Q.F. Xing, R.B. Yu, J. Meng, J. Chen, G.R. Liu, Hydrothermal synthesis of ZrW_2O_8 nanorods, Physica B 371 (2006) 81–84.
[15] U. Kameswari, A.W. Sleight, J.S.O. Evans, Rapid synthesis of ZrW_2O_8 and related phases, and structure refinement of $ZrWMoO_8$, Int. J. Inorg. Mater. 2 (2000) 333–337.
[16] Q.F. Xing, X.R. Xing, R.B. Yu, L. Du, J. Meng, J. Luo, D. Wang, G.R. Liu, Single crystal growth of ZrW_2O_8 by hydrothermal route, J. Cryst. Growth 283 (2005) 208–214.
[17] J. Yang, Q.Q. Liu, X.J. Sun, G.F. Xu, X.N. Cheng, Synthesis of negative thermal expansion materials $ZrW_{2-x}Mo_xO_8(0 \leq \times \leq 2)$ using hydrothermal method, Ceram. Int. 35 (2009) 441–445.
[18] J.S.O. Evans, Z. Hu, J.D. Jorgensen, D.N. Argyrious, S. Short, A.W. Sleight, Compressibility, phase transitions and oxygen migration in the zirconium tungstate ZrW_2O_8,, Science 275 (1997) 61–65.
[19] A.W. Sleight, Compounds that contract on heating, Inorg. Chem. 37 (1998) 2854–2860.
[20] A.K.A. Pryde, K.D. Hammonds, M.T. Dove, V. Heine, J.D. Gale, M.C. Warren, Origin of the negative thermal expansion in ZrW_2O_8 and ZrV_2O_7, J. Phys.: Condens. Matter 8 (1996) 10973–10982.
[21] Y. Yamamura, T. Tsuji, K. Saito, M. Sora, Heat capacity and order–disorder phase transition in negative thermal expansion compound ZrW_2O_8, J. Chem. Thermodynam. 36 (2004) 525–531.
[22] Y. Yamamura, N. Nakajima, T. Tsuji, Heat capacity anomaly due to the α-to-β structural phase transition in ZrW_2O_8, Solid State Commun. 114 (2000) 453–455.
[23] M.R. Hampson, J.S.O. Evans, P. Hodgkinson, Characterization of oxygen dynamics in ZrW_2O_8, J. Am. Chem. Soc. 127 (2005) 15175–15181.
[24] T. Varga, C. Lind, A.P. Wilkinson, H. Xu, C.E. Lesher, A. Navrotsky, Heats of formation for several crystalline polymorphs and pressure-induced amorphous forms of AMo_2O_8 (A = Zr, Hf) and ZrW_2O_8, Chem. Mater. 19 (2007) 468–476.
[25] K.D. Buysser, I.V. Driessche, B.V. Putte, P. Vanhee, J. Schaubroeck, S. Hoste, Study of negative thermal expansion and shift in phase transition temperature in Ti^{4+}- and Sn^{4+}-substituted ZrW_2O_8 material, Inorg. Chem. 47 (2008) 736–741.